Problems of Crystallization of B2-FeAl Based Alloys

Jaromír Kopeček [1, a], Karel Jurek [2,b], Vladimír Šíma [3,c] and Pavel Lejček [1,d]

[1] Dept. of Metals, Institute of Physics of AS CR, Na Slovance 2, 182 21Praha 8, Czech Republic

[2] Dept. of Structure Analysis, Institute of Physics of AS CR, Cukrovarnická 10, 162 53 Praha 6, Czech Republic

[3] Dept. of Physics of Materials, Charles University, Ke Karlovu 5, 121 16 Praha 2, Czech Republic

[a] kopecek@fzu.cz, [b] jurek@fzu.cz, [c] sima@met.mff.cuni.cz, [d] lejcekp@fzu.cz

Keywords: Fe-40Al, iron aluminides, carbides, crystal growth

Abstract. The aim of this study was to clarify the sources of brittleness in the B2 based Fe–40 at.% Al alloys. The fracture behavior of these alloys is complex even at room temperature and is affected by the ternary additions. Although the main source of the grain boundary weakness in FeAl arises from environmental embrittlement, important source seems to be of the intrinsic nature. The star cracks aggregates and voids were found in the conventionally cast and rolled materials. The single crystals prepared by Bridgman method contain the star cracks when grown with growth rates higher than 9 mm/h. At lower growth rates the stress induced by solidification is not high enough to cause crack initiation at the interfaces of the Fe_3AlC carbide precipitates. It was found that another way to remove solidification stresses is the ultrasound forced casting.

Introduction

B2 based iron aluminides have been considered to be the metallurgical challenge for decades. The excellent oxidation and sulphidation resistance at high temperatures, low density and low raw material cost are balanced with poor ductility at low temperatures and creep properties, which didn't allow metallurgists to use standard methods of materials preparation [1]. Up to now the applied iron aluminides are prepared either by quite complicated powder metallurgy [2] or by precise casting [3]. In the last decades different scientific groups have been attempting to prepare and process the alloy using cheap additives or cheap standard technology at least.

Iron aluminides exhibit the anomaly of the yield stress at ~ $0.4T_M$ in both ordered structures $D0_3$ and B2. The anomaly was successfully explained by thermal vacancies strengthening model of George and Baker [4], who described the processes running even in other parts of the temperature dependence of the yield stress. The later study of the orientation dependence of the yield stress anomaly supports this model [5]. It is obvious that the quenched state in this material can enhance the low temperature brittleness only, as the excess thermal vacancies recover at high temperatures, where material use is expected. The effect of the quenched non-equilibrium B2 long range order parameter is the same. It shows that the ways how to modify the intrinsic properties of the binary alloy are quite limited (the material would be used at the temperatures, where thermally activated processes could not be neglected).

The additional elements or the strengthening particles are used for modifying the binary iron aluminides. The use of the precipitates created by the elements like carbon combines both these ways. Carbon creates double carbide Fe_3AlC with perovskite structure (κ-phase) or graphite as its solubility limit in iron aluminides is around 1 at. % [6]. The details of the phase equilibrium surrounding the area of interest were studied frequently [6-9]. The structural formula Fe_3AlC should be understood more like a label, because the real content of carbon also differs from the stoichiometry $Fe_3AlC_{0,5}$ and could be described as $Fe_{4-y}Al_yC_x$ [9].

The double carbides with perovskite structure have interesting mechanical properties at general and the materials with the stoichiometry Fe_3AlC were studied as well [10]. Fe_3AlC form the most common precipitates in the B2-based Fe- 40 at.% Al alloys, but following the phase diagram, we can expect the presence of graphite, too [7-9]. Fe_3AlC carbide improves the room temperature strength and ductility and its interfaces act as traps for hydrogen, which cause environmental embrittlement [11,12].

Experimental details

The composition of the used alloys is Fe- 39.20 at. % Al - 1.00 at. % C - 0.05 at. % Si for the material marked Fe-40Al-1C and Fe - 40.48 at.% Al - 0.11 at.% C - 2.66 at.% Ti - 0,11 at. % Si for the material marked Fe-40Al-3Ti. The composition of the alloy was checked by standard chemical analysis. The samples were chill cast in vacuum. As-cast materials were annealed 2 hours at 900°C followed by 2 hours at 1200°C. Fe-40Al-1C was than hot rolled at1200°C, Fe-40Al-3Ti was cooled slowly on the air.

The high-power ultrasound source used for preparation of some samples had power of 800 W and frequency of 40 kHz.

The monocrystals were prepared using the Bridgman method in the Granat-74 apparatus. The floating zone method was performed in the furnace with optical heating FZ-T-1200-X-VI-VP. The monocrystals were grown under argon atmosphere in both cases. The growth rates are mentioned at description of particular samples.

The Auger electron spectroscopy (AES) measurements were performed at ferrite grain boundaries by means of a CAMECA Riber (MAC 3) apparatus at Ecole Nationale Supérieure des Mines de St. Etienne, France. The specimens cooled using liquid nitrogen were broken by in-situ impact bending in an ultra-high-vacuum chamber of ca 10^{-7} Pa and studied immediately with a primary electron beam of a voltage of 10 kV. The lateral resolution of the analyzed spot was of the order of few μm^2 and the analyzed depth was few atomic layers at the fracture surface.

The optical microscopy was performed using Zeiss ZM1 microscope with circular polarized light and the scanning electron microscopy (SEM) on JXA-733 with the EBSD detector produced by EDAX. The diffractometer X´Pert Pro was used for X-rays diffraction analysis (XRD) of bulk samples in Bragg-Brentano geometry.

Results

A set of the samples showed the standard problematic phenomenons, which are the large grains (average grain diameter was over one millimeter), the shrinkage cavities and the cracks connected into the asterisks. The attempts to roll the sample led to massive intercrystalline cracking, Fig. 1. The microstructure of the rolled sample is shown in Fig. 2. There are visible the mentioned shrinkage cavities, asterisk cracks and Fe_3AlC precipitates, which have polygonal, convex shape and create rounded lines of individual precipitates or long straight rectangular shape. The long cracks on the grain boundaries are enlarged by rolling, but some of them - the cavities and asterisk cracks - are present before high-temperature deformation. The structure is homogenous in the sense of the distribution of precipitates and both composition of precipitates and matrix.

As the rolling caused extended cracking, we decided to apply AES study of the fracture surfaces of the interfaces to look for the segregation of harmful elements reducing the cohesion of grain boundaries, but there were not found any other element besides those forming the alloy. The formulas taking into account long-range order of the alloy was used to evaluate the Auger spectra [13]. The grain boundary composition of 38.7 at. % Al and 15.5 at. % C is in principal agreement with the knowledge about the segregation in the ordered alloys: The stronger is ordering the weaker is interfacial segregation. Rather high concentration of carbon may reflect several effects: Its grain

boundary segregation, presence of carbide precipitates there and the result of the contamination of the fracture surface from the residual gas atmosphere in the AES apparatus. Therefore, this value cannot be ascribed exclusively to carbon segregation. Segregated carbon is presented in the form of graphite at the grain boundaries. Graphite was observed by XRD but not by SEM. It was confirmed by XRD that Fe-40Al-1C consists from FeAl (a = 2.899 Å), Fe_3AlC (a = 3.747 Å) and small amount of graphite, which is supposed that graphite also creates small globular or lamellar precipitates, predominantly at the grain boundaries [7,8]. The quantitative analysis of XRD spectra is tricky as big grains introduce bad statistics due to extinction and texture.

Figure 1 The Fe-40Al-1C chill cast ingot after an attempt to roll contains massive intercrystalline cracks.

Figure 2 Microstructure of the cross-cut of the rolled sample Fe-40Al-1C. Optical microscopy.

There was not found any extrinsic harming of the studied material in the rolled sample. All of the observed features must then arise from the intrinsic nature of the Fe-40Al-1C material. As the intergranullar cracks occur in the material during rolling itself, we focused more to the behavior of monocrystalline samples to understand mainly the origin of asterisk cracks.

Figure 3 Asterisk cracks and Fe_3AlC precipitates in the monocrystal Fe-40Al-1C grown by the Bridgman method.

Figure 4 Detail from optical microscope showing the cracks nucleating at the interfaces of precipitates and matrix in the monocrystal Fe-40Al-1C grown by the Bridgman method.

Monocrystals of Fe-40Al-1C grow quite easily by Bridgman method. The monocrystal that was grown with the rate 28 mm/h have very similar or even the same structure as the rolled sample in grain interiors, Fig. 3. The crystal contains the network of Fe_3AlC precipitates and bunches of black objects - the cracks. The cracks sometimes form the asterisks. As the orientation of the grow axis

perpendicular to the polished cut is <001>, it means that the asterisk cracks are perfectly crystalographically located along the <001> and sometime even <011>.

The detail view in Fig. 4 shows the core of asterisk crack. The cracks of this kind do not possess crystalographically defined centre. SEM image in Fig. 5 shows other example of the asterisks cores, which confirms an idea that the cracks in the interior of the grain nucleate at the interfaces between the Fe_3AlC carbides and the B2 ordered FeAl matrix.

The EBSD method proved very good monocrystallinity of the sample grown by the Bridgman method with the rate 28 mm/h. The orientation dispersion is less than 3° and the crystal diameter is 2 cm. The detail of the orientation map surrounding the asterisk crack surprisingly does not show the splays at the edges of the cracks. It supports an idea, that these cracks are kind of the defects like shrinkage cavities caused by contraction of the melt during quick solidification. The carbide particles are not visible at this map, because the structures of both phases are very similar in the diffraction image.

The monocrystal that was grown with the rate of 9 mm/h verifies the above findings. Its structure does not contain even the small cracks and the structure of the precipitate network is finer, Fig. 7. The structure of the precipitation lines formed by small rectangular or rhombic grains is the same as in previous cases, Fig. 8. The XRD confirms the presence of the Fe_3AlC precipitates, but their stoichiometry is shifted from the ideal ratio 3:1 for Fe:Al: The measured amount of aluminum in precipitates is (30 ± 1) at. %, whether there is (39 ± 1) % of alumina in the matrix in accordance with the chemical analysis.

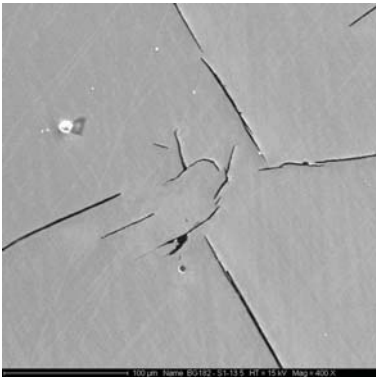

Figure 5 The core of the asterisk crack in Fe-40Al-1C. SEM image.

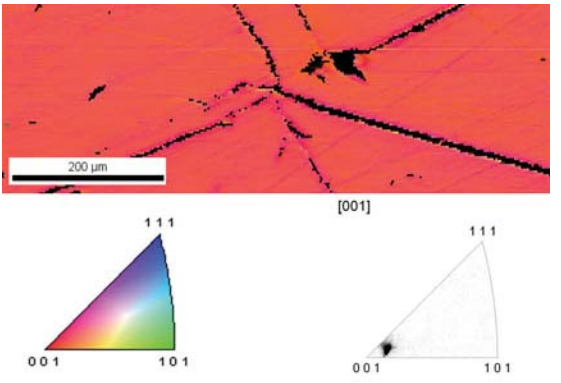

Figure 6 The EBSD image of the core of the asterisk crack in Fe-40Al-1C material. The colors correspond to the orientation triangle left bottom, particular orientations from the map are pointed in the triangle right bottom.

The EBSD results show the similar picture as in the previous case. The Fe_3AlC precipitates do not cause splaying of the surrounding matrix. The recognition of the respective structures just by EBSD is nearly impossible as both phases have similar cubic structure. Moreover, Fe_3AlC precipitates are little bit damaged during the sample polishing and the quality of back scattered electron picture is not perfect and hence the image quality is low, Fig. 9.

The orientation of the monocrystal that was grown with the rate of 9 mm/h is close to the <521> direction. Similar type of orientation from the middle of the orientation triangle - <531> - was

already observed in the case of Fe - 28 at. % Al - 4 at. % Cr intermetallics [14]. There is the tendency to create subgrains, but the misorientation is low.

The Bridgman monocrystal that was grown with the rate of 9 mm/h was used as a seed for the floating zone method and monocrystal was prepared with the growth rate of 10 mm/h. The distribution of the precipitates is similar for both growth processes. There are no cracks. The subgrains in the material prepared by the floating zone enhance their misorientation up to 12°, as a consequence of the development of the existing subgrain structure in the seed prepared by the Bridgman method.

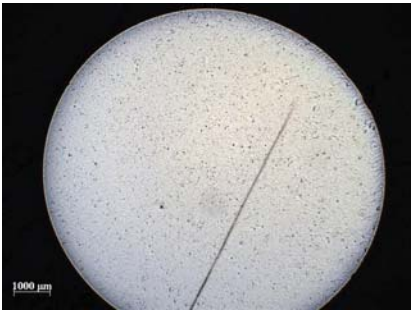

Figure 7 Fe-40Al-1C, the monocrystal prepared by the Bridgman method with the growth rate of 9 mm/h.

Figure 8 Detail of Fig. 7 shows the Fe_3AlC rectangular precipitates connected into the rounded or straight patterns.

To improve the quality of the prepared monocrystals, an ultrasound forced mould was constructed and installed in the vacuum furnace. The energy transmitted into the solidifying alloy by transducer helps to recover the local stress fields. The ultrasound forced sample did not contain any shrinkage cavities and cracks after the solidification. The average grain size was slightly smaller in ultrasound forced samples than in the conventionally solidified ones. The Fe_3AlC carbides fill the grains interiors but are clearly visible even at grain boundaries, Fig. 10. The morphology of the precipitates is similar to that in previous cases.

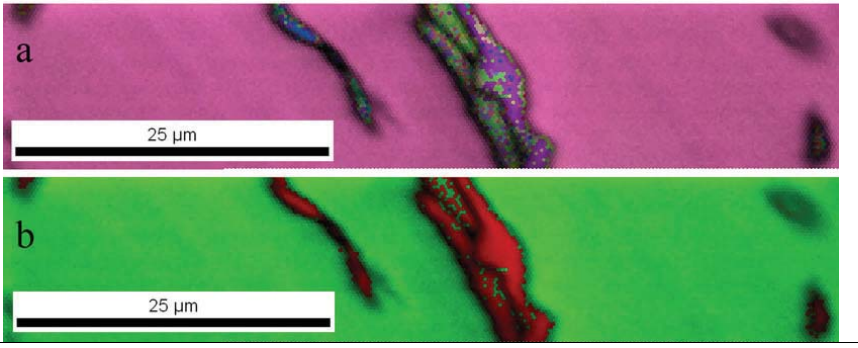

Figure 9 Monocrystal of Fe-39Al-1C that was grown by Bridgman method with the rate of 9 mm/h. a) The EBSD orientation image. The color scale of both phases is the same as in Fig. 6. b) The EBSD phase image. Green color belongs to B2-FeAl, red color to Fe_3AlC carbide.

The minor part of the work was done on the Fe-40Al-3Ti material. The as-cast structure after quenching contains long intergranullar cracks, shrinkage cavities and small rectangular or triangular precipitates of TiC, Fig. 11. The structure is homogenous with respect to both composition and orientation. AES showed the concentrations of 40.9 at. % Al and 2.5 at. % Ti. The first value is slightly higher than is the bulk composition and the second one is slightly smaller. There is no any strong tendency to the grain boundary segregation, like in the case of Fe-40Al-1C. Titanium is dissolved in the matrix; the part of its volume is in the carbides.

The possibility to prepare monocrystal from this material by the seedless floating zone method was tested, but the grain boundaries parallel to the growth direction are very stable and the structure of

Figure 10 The as-cast material Fe-40Al-1C solidified under the ultrasound power of 800W.

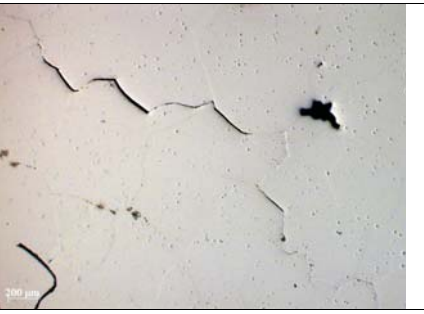

Figure 11 The as-cast material Fe-40Al-3Ti cooled on the air contains cracks, shrinkage cavities and small TiC precipitates in the grains interiors.

prolonged grains was obtained, Fig. 12. The growth direction of the respective grains varied between <311> and <211>.

Figure 12 Fe-40-3Ti materials that was grown by the seedless floating method with growth rate 10 mm/h. The grain boundaries parallel to the growth direction are very stable in this material. Some grains were broken out during preparation of the cross-cut. The growth started at the right hand side.

Discussion

Two types of the cracks were discovered during the experiments with the B2-FeAl alloys. One type represents long intergranular cracks caused by environmental embrittlement and following shock stresses during cooling or rolling. This type of cracks exists in both studied materials already after annealing, but hot rolling enhances their presence.

If the materials are cast in vacuum, the cracks caused by hot rolling originating from the shock stresses between cold sheet roll and hot iron aluminides can be suppressed by the ingot protective bandage. Detail of the ingot covering process will be described elsewhere [15] and the results of the mechanical testing were already published [16,17].

There are not the cracks caused by rolling only, another important source of the fatal cracks in the carbides reinforced iron aluminides is the casting process itself. During solidification the stress arises at the phase interface between B2-FeAl matrix and Fe_3AlC carbides. If the stress is high enough, the crack initializes at the interface and consequent changes in the stress field result in the formation of the crack bunches followed by the asterisk cracks in the matrix surrounding the precipitates.

The grown monocrystals showed that the small cracks in the interior of the grain originate from the thermal stresses during solidification and can be removed either by very slow cooling performed here by Bridgman method or by forcing of solidifying melt by ultrasound vibrations. The second method was found to be successful for materials preparation.

Of course, the crucial problem is the control of the elements mainly causing the embrittlement like is hydrogen, which could not be proved by any of used analytical method. Just the possibility to roll the materials cast in vacuum justifies us to mark the cracking on the interfaces of carbide and matrix as an intrinsic property.

The question of the selection of the easy growth direction remains open. When the monocrystal is prepared by Bridgman method using growth the rate of 28 mm/h, the orientation of the nucleated grain is close to the <001> direction. When the monocrystal is prepared using slower growth rates (despite the technique used), the growth direction changes to more general directions from the middle of the orientation triangle.

The work will continue with the study of fracture surfaces from monocrystalline samples and deeper research of the distribution of Fe_3AlC carbides and their orientation to the matrix.

Summary

The B2-based Fe - 40 at. % Al alloys with small additions of carbon or titanium are potentially very interesting materials, the application of which is limited by low temperature brittleness and strong tendency to cracking. The thermal stresses at the interfaces of Fe_3AlC carbides and B2-ordered matrix was confirmed to be the reason of the asterisk cracks in the grain interiors. The ultrasound forcing of solidifying melt is equivalent to very slow cooling during Bridgman method growth of monocrystals and can be applied to material preparation. It seems that the long intergranullar cracks can be suppressed by vacuum casting and by the protective covering of the ingots before rolling to prevent environmental embrittlement and nucleation of shock cracks.

Acknowledgement

Authors would like to thank the Czech Science Foundation for the support through the grant 106/06/0019. The authors wish to thank Mr. Pierre Passet (ESME, St. Etienne, France) for technical assistance in AES measurements.

References

[1] I. Baker, P.R. Munroe: Int. Mater. Rev., Vol. 42 (1997), p. 181

[2] D.G. Morris, S.C. Deevi: Mater. Sci. Engn. A, Vol. 329-330 (2002), p. 573

[3] P. Kratochvíl: Intermetallics, Vol. 16 (2008), p. 578

[4] E.P. George, I. Baker: Philos. Mag. A, Vol. 77 (1998), p. 737

[5] D. Wu, I. Baker, P.R. Munroe, E.P. George: Intermetallics, Vol. 15 (2007), p. 103

[6] L. J. Huetter, H. H. Stadelmaier: Acta Met., Vol. 6 (1958), p. 367

[7] I. Jung, G. Sauthoff: Z. Metallkd., Vol. 80 (1989), p. 490

[8] M. Palm, G. Inden: Intermetallics, Vol. 3 (1995), p. 443

[9] W. Sanders, G. Sauthoff: Intermetallics, Vol. 5 (1997), p. 361

[10] W. Sanders, G. Sauthoff: Intermetallics, Vol. 5 (1997), p. 377

[11] L. Pang, K. S. Kumar: Acta Mater., Vol. 46 (1998), p. 4017

[12] A. Radhakrishna, R.G. Baligidad, D.S. Sarma: Scripta Mater., 45 (2001), p. 1077

[13] P. Lejček, O. Schneeweiss: Surface Sci., Vol. 487 (2001), p. 210

[14] J. Kopeček, P. Lejček: J. Cryst. Growth, Vol. 287 (2006), p. 267

[15] V. Šíma, P. Kozelský, P. Hána: submitted to International Journal of Materials Research (2008)

[16] P. Kudrna: Diploma thesis, FJFI ČVUT, Praha (2008)

[17] P. Haušild, M. Karlík, A. Kubošová and P. Kudrna, in: *Porušování a design materiálů*, Ústav fyziky materiálů AV ČR, Brno (2007), p. 157